Astron. Astrophys. 342, 881–891 (1999)

ASTRONOMY AND ASTROPHYSICS

Uncertainties in the solar system r-abundance distribution⋆

S. Goriely

Institut d'Astronomie et d'Astrophysique, C.P. 226, Université Libre de Bruxelles, bd. du Triomphe, B-1050 Brussels, Belgium

Received 4 September 1998 / Accepted 22 October 1998

Abstract. The solar system r-abundance distribution is commonly derived from the observed solar values by subtracting the possible nucleosynthetic contribution of the s-process. The new parametric model of the s-process called the canonical multi-event model is used to derive the s-component of the solar abundance distribution and to study the impact of nuclear and observational uncertainties on the solar r-abundance distribution.

Key words: nuclear reactions, nucleosynthesis, abundances – Sun: abundances – solar system: general – stars: abundances

1. Introduction

For the last decades, an extremely intense amount of work has been devoted to the study of the rapid and slow neutron-capture processes of nucleosynthesis (known as the r- and s-processes, respectively) called for to explain the origin of the vast majority of the elements heavier than iron observed in nature (e.g Seeger et al. 1965). Though both processes invoked neutron captures on light seed nuclei to produce the heavy elements, they take place in completely different astrophysical environments and on very different time scales. The s-process nucleosynthesis results from a relatively weak neutron production (characterized by neutron densities of about $N_n \simeq 10^8\,\mathrm{cm}^{-3}$) and from their captures by pre-existing nuclei (most importantly iron, assumed to be produced in previous stellar generations) on time scales long compared with most β-decay lifetimes (i.e larger than a few years). On the contrary, the r-process neutron captures are believed to take place in a high-neutron-density environment ($N_n \gtrsim 10^{20}\mathrm{cm}^{-3}$) on time scales of about 1 second. In this case, neutron captures are faster than β-decay rates and the nuclear flow drives seed nuclei into the very neutron-rich region of the nuclear chart.

Although the modelling of the s-process still faces some problems–especially concerning the identification of the astrophysical sites in which it might develop–our understanding of the nuclear mechanisms responsible for the production of the s-nuclei can be regarded as very satisfactory, at least in comparison with the r-process. One of the major reasons of this success consists in the remarkable effort performed in experimental and theoretical nuclear physics to determine as reliably as possible the nuclear quantities of importance to the s-process nucleosynthesis. Most of the nuclei involved in the s-process have been studied in the laboratory, and a large number of their properties are known experimentally. Some specific nuclear uncertainties obviously remain, because of the special thermodynamic conditions found in stellar environment which cannot be reproduced in terrestrial laboratories and because of the still unknown properties of some of the β-unstable nuclei produced along the s-process path. As regards the astrophysical modelling, the situation is unfortunately much more cumbersome. The so-called realistic s-process models aim at describing through consistent stellar models the burning phases where the astrophysical conditions required for the s-process to take place are fulfilled. Even though the observation of the radioactive Tc in stellar envelopes clearly proves that the s-process takes place during hydrostatic burning phases of a star, it remains difficult to explain the origin of the large neutron concentrations required to produce s-elements. At the present time, two nuclear reactions are suggested as possible neutron sources, $^{13}\mathrm{C}\,(\alpha\,,\mathrm{n})\,^{16}\mathrm{O}$ and $^{22}\mathrm{Ne}\,(\alpha\,,\mathrm{n})\,^{25}\mathrm{Mg}$. These reactions could be responsible for a large production of neutrons during given burning phases, namely the core He-burning of massive stars ($M \geq 10\,\mathrm{M}_\odot$) (e.g Langer et al. 1989; Prantzos et al. 1990; Baraffe et al. 1992) and the shell He-burning during the thermal AGB instabilities (well-known as thermal pulses) of low and intermediate mass stars ($M \leq 10\,\mathrm{M}_\odot$) (e.g Malaney & Boothroyd 1987; Holowell & Iben 1989; Straniero et al. 1995). Even though the core He-burning has proved its ability to produce the lightest s-elements (i.e $70 \lesssim A \lesssim 90$), the astrophysical models underlying the thermal pulse scenario (believed to be responsible for the production of the $A > 90$ s-elements) are still quite uncertain, in particular in the description of the mechanisms that could be at the origin of the neutron production (e.g Lattanzio 1989; Frost & Lattanzio 1995). For this reason, the models are often artificially parametrized in order to increase the neutron concentration (e.g. Busso et al. 1992).

At the opposite of the s-process, the r-process remains poorly understood in many respects. Its study requires the knowledge of

⋆ Tables 1 and 2 are only available in electronic form at the CDS (Strasbourg) via anonymous ftp to cdsarc.u-strasbg.fr (130.79.128.5) or via http://cdsweb.u-strasbg.fr/Abstract.html

Correspondence to: sgoriely@astro.ulb.ac.be

a large body of nuclear physics and astrophysics information. On the nuclear physics side, the nuclear structure properties (such as the nuclear masses, deformation, ...) of thousands of nuclei located between the valley of β-stability and the neutron drip line have to be known, as well as their interaction properties, such as the (n,γ) and (γ,n) rates, α- and β-decay half-lives and the fission probabilities. Despite much recent experimental efforts, those quantities for most of the nuclei involved in the r-process remain unknown. On top of these nuclear difficulties, the question of the astrophysical conditions under which the r-process can develop is far from being settled. The site(s) of the r-process is (are) not identified yet, all the proposed scenarios facing serious problems (Arnould & Takahashi 1998). In particular, the neutrino-energized low-density and hot wind (the so-called hot bubble) streaming out of the neutron star forming at the centre of a Type-II supernova seems now to be unable to provide suitable conditions for the development of an r-process (Qian & Woosley 1996; Takahashi & Janka 1997).

In addition to the neutron-capture processes, another nucleosynthetic process (the p-process) is invoked to explain the origin of most of the neutron-deficient isotopes with charge number $Z \geq 34$ (referred to as the p-nuclei) which cannot be synthesized by the s- or r-processes. The p-nuclei represent no more than 1% to 0.1% (with increasing Z) of the bulk $Z \geq 34$ elemental abundances, made predominantly of nuclei produced by the s- and r-processes. The production of the p-nuclei can be explained by the transformation of pre-existing seed nuclei (produced by the s- and r-processes) mainly by neutron photodisintegration or radiative proton captures on the lightest nuclei. It seems now astrophysically plausible that the p-nuclei originate from the oxygen/neon layers of highly evolved massive stars during their pre-supernova phase (Arnould 1976), or during their explosion either as Type II supernovae (Rayet et al. 1995) or even as pair-creation supernovae (Rayet et al. 1993).

About 30 nuclei heavier than iron, the so-called s-only isotopes, are exclusively synthesized during the low-neutron-densities events characteristic of the s-process. They are indeed shielded from the r-process production by the existence of a lighter isobaric element. In contrast, most of the neutron-rich stable isotopes cannot be produced by the s-process and the high neutron densities found in the r-process are called for to explain their origin. They are named r-only nuclei. In addition to these s-only and r-only nuclei, a large number of stable nuclides (called sr-isotopes) are produced by both processes and the remaining neutron-deficient nuclei almost exclusively by the p-process. In order to understand the 3 very different s-, r- and p-nucleosynthetic mechanisms, it is of first importance to decompose the global abundance distribution observed in the solar system into its s-, r- and p-components. Due to the large nuclear physics and astrophysics uncertainties related to the r-process, the s-contribution to the isotopic solar abundances is usually derived from theoretical s-process calculations, while the r-process contribution is subsequently deduced by a simple subtraction of the s-contribution from the observed solar value. To do so, fully parametric s-process models, free of all astrophysical constraints, are considered in order to avoid the difficulties remaining in the astrophysical modelling of the s-process site. Such parametric models have the virtue to give very accurate fit to the solar abundances of the s-only elements, and consequently to enable a precise extraction of the s-component from the solar abundance of the sr-nuclei. Finally, the r-component is obtained by subtracting this s-contribution from the solar value. To estimate the p-component, a similar approach can be conducted, though an alternative procedure consists of estimating the p-component from realistic p-process calculation (e.g. Rayet et al. 1995) and subtracting the p-contribution from the solar abundances before starting with theoretical s-process calculations. Such a procedure is followed for example by Käppeler et al. (1989), but not in the present paper. The parametric s-process model are indeed able to explain remarkably well the solar abundances of the s-only nuclei (within a few percents), in contrast to the realistic p-process models which are still affected by astrophysical, as well as nuclear physics uncertainties, so that it remains difficult to determine safely the exact isotopic p-contribution to the solar system content.

The most popular of the parametric s-process models, well-known as the classical or exponential model, is based on the original canonical model of Burbidge et al. (1957) and was first successfully developed by Clayton et al. (1961). The canonical model assumes that some stellar material composed of iron nuclei only is subjected to neutron densities and temperatures that remain constant over the whole time scale of the neutron irradiation. In addition, the classical model assumes that the solar system s-abundance pattern originates from a superposition of 3 exponential distributions of the time-integrated neutron exposure, defined as $\tau = \int_0^t N_n v_T dt$ (where v_T is the most probable relative neutron-nucleus velocity at the temperature T). The 3 exponential distributions are traditionally referred to as the weak component (responsible for the production of the $70 \leq A \leq 90$ s-nuclei), the main component (for the $90 \leq A \leq 204$ isotopes) and the strong component (for the $A > 204$ nuclides). Since the exponential model has been very successful in reproducing the solar s-abundance distribution, it has been extensively used to derive the solar r-abundances. However, such a theoretical estimate of the solar s-abundance distribution is not free from uncertainties. The classical model is affected by uncertainties related to observational and nuclear input data, but also with theoretical shortcomings inherent to the canonical exponential approach. In particular, the influence of the fundamental assumption made in the classical model regarding the predefined exponential form of the exposure distributions can be questioned. In addition, the way the nuclear and observational uncertainties within the s-process model affect the derived solar r-abundance distribution is difficult to estimate within the classical approach. For this reason, systematic errors on the solar r-abundances are rarely evaluated. In order to test the influence of the assumptions made in the exponential approach, a new s-process model has been developed recently (Goriely, 1997). In Sect. 2, this so-called multi-event s-process is reviewed and compared with the classical model predictions. This comparison emphasizes the influence of the hypothesis made in the classical model concerning the exponential exposure distribu-

tion. A major advantage of the multi-event approach is also to enable a systematic study of the various uncertainties affecting the parametric canonical s-process models. In Sect. 3, the different uncertainties related to the input data to the s-process models are estimated and discussed. These concern uncertainties in observed solar abundances and nuclear data (the radiative neutron capture and β-decay rates). A special care is given to the nucleosynthesis in the Pb region by considering the possible absence of the strong component of the s-process. The impact of all these uncertainties on the derived solar s- and r-abundance distributions is studied in detail. The final r-contribution to the solar abundances is given with estimated error bars.

2. The multi-event s-process model

The multi-event s-process is defined as a superposition of a given number of canonical events taking place in different thermodynamic conditions. Each canonical event is characterized by a given neutron irradiation on the ^{56}Fe seed nuclei during a time t at a constant temperature T and a constant neutron density N_n. The combination of s-process events that provides the best fit to the solar abundances is derived with the aid of an iterative inversion procedure described in Goriely (1997). In contrast to the classical model which assumes a superposition of exponentially decreasing exposures, the multi-event model makes no hypothesis concerning any particular pre-defined exposure distribution. By considering a set of astrophysically plausible events, an optimized s-abundance curve is derived by the iterative inversion method, along with the corresponding exposure distribution. For each event, a full network calculation including 640 nuclei between Cr and Po is solved to derive the abundances. The latest experimental neutron capture cross sections are used (Bao & Käppeler 1987; Beer et al. 1992; Wisshak et al. 1995, 1996, 1998; Beer et al. 1997 and references therein). When not available, the cross sections are calculated within the statistical Hauser-Feshbach (HF) model (called MOST for Modèle Statistique, Goriely 1998b). The HF calculation is also used systematically to deduce from the laboratory neutron capture cross sections the stellar rates by allowing for the possible thermalization of low-lying states in the target nucleus. Note that the non-thermalization of the isomeric state in ^{85}Kr and ^{180}Ta, as well as the thermalization of ^{115}In and ^{176}Lu at temperatures exceeding $T_8 \simeq 2.5$[1] and $T_8 \simeq 3$, respectively, are introduced explicitly in the reaction network (Käppeler et al. 1989; Nemeth et al. 1994). The β-decay and electron capture (EC) rates in stellar conditions are taken from Takahashi & Yokoi (1987). The (n,α) and (γ,α) reactions on the Bi and Po isotopes (as well as ^{146}Sm) are also included.

For a given set of nuclear physics data, two degrees of freedom appear in the multi-event approach, namely the range of allowed thermodynamic conditions (such as the temperature, the neutron density and the irradiation time) and the set of nuclei the inversion method is supposed to fit (or equivalently the set of nuclei the s-process is expected to produce). The sensitivity of the multi-event s-process model to these two degrees of freedom was studied in Goriely (1997). Since in the present paper, we are principally concerned with the uncertainty study, the following choices are made. With respect to the set of nuclei the s-process should produce in solar abundances, we consider here the s-only nuclei which cannot be produced by any other known nucleosynthetic process. In addition to the s-only isotopes, we also include ^{208}Pb (predicted to be produced by the strong s-process component) and ^{86}Kr and ^{96}Zr (largely produced by the s-process). ^{152}Gd or ^{164}Er are also included, because of the inability of the p-process and the capacity of the s-process to produce them in solar abundance (Goriely 1997). The resulting set is made of 35 nuclei. As regards the astrophysical conditions in which the s-process events are allowed to take place, we consider temperatures in the $1.5 \leq T_8 \leq 4.0$ range and neutron densities in the $7.5 \leq \log N_n[\mathrm{cm}^{-3}] \leq 10.0$ range. These conditions are indeed astrophysically plausible (Käppeler et al. 1989). Each of the 121 (T_8, N_n) events evenly distributed in grid steps of 0.25 in T_8 and $\log N_n[\mathrm{cm}^{-3}]$ are assumed to take place at 40 different irradiation times corresponding to 40 evenly distributed values of n_{cap} in the $5 \leq n_{cap} \leq 150$ range, where

$$n_{cap}(t) = \sum_{Z,A} A\, N_{Z,A}(t) - \sum_{Z,A} A\, N_{Z,A}(t=0) \qquad (1)$$

is the number of neutrons captured by the seed nuclei during the irradiation time t. A unique electron density $N_e = 10^{27}$ cm^{-3} characteristic of the AGB He-burning phase is taken to estimate the EC rates.

The solar abundances as well as the decomposition into s- and r-components predicted by the classical model are taken from the compilation of Palme & Beer (1993) which is in close agreement with the popular work of Anders & Grevesse (1989) for most of the elemental abundances except for some elements, like Se or Au, for which recent revised measurements are used by Palme & Beer (1993).

Figure 1 shows that the multi-event model can give an excellent fit to the solar system abundances of the s-only nuclei. This calculation is referred to as our standard calculation when no uncertainty is considered. The quality of the fit can be quantitatively expressed by a root mean square deviation factor, f_{rms}, between the calculated (N_{cal}) and the observed ($N_\odot$) abundances, and defined by

$$f_{rms} = \exp\left[\frac{1}{n_{tot}} \sum_{Z,A}^{n_{tot}} \ln^2 \frac{N_{cal}(Z,A)}{N_\odot(Z,A)}\right]^{1/2}, \qquad (2)$$

where the sum runs over the $n_{tot} = 35$ s-only nuclei (of charge Z and atomic mass A) introduced in the fitting procedure. Our standard calculation gives a factor $f_{rms} = 1.10$ very close to unity. The multi-event predictions are also in good agreement with the exponential model predictions of Palme & Beer (1993). In particular, both models show similar discrepancies with respect to the solar observations, for example a 20% underabundance of ^{116}Sn, or an overabundance of elements like Pt. Improvements with respect to the classical model (which is characterized by $f_{rms} = 1.44$) can also be seen in the pre-

[1] where T_8 is the temperature expressed in 10^8K

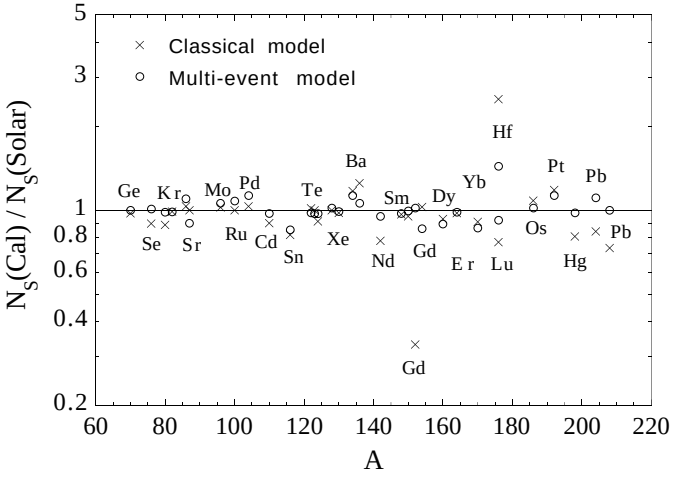

Fig. 1. Ratio of the calculated to the solar system abundances of the s-only nuclei. The multi-event predictions (circles) are compared with the classical model predictions (crosses) of Palme & Beer 1993.

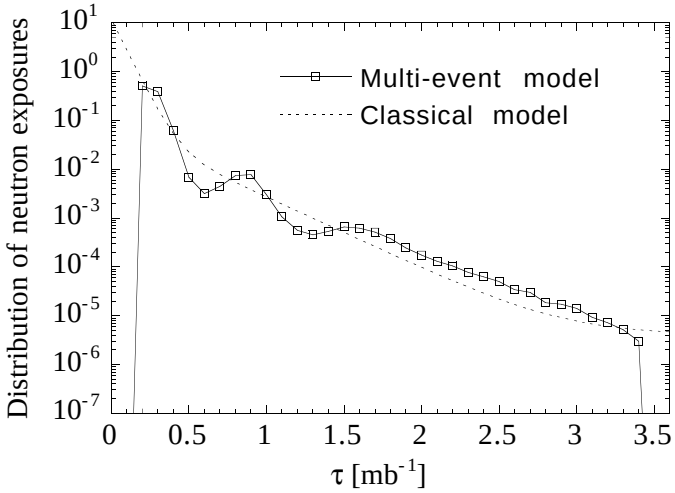

Fig. 2. Distribution of the neutron exposures τ characterizing the events involved in the abundance fit of Fig. 1. The exponential exposure distribution predicted by the classical model of Beer et al. (1997) is also shown for comparison.

diction of the abundances of ^{142}Nd, ^{152}Gd, ^{134,136}Ba or elements heavier than Lu. The better agreement is essentially due to updated experimental or theoretical reaction rates, as well as a higher degree of sophistication in the multi-event model as compared with the exponential approach. Note that some deviations between the multi-event and exponential models are unavoidable since neither the nuclear physics input (especially the calculated neutron capture rates), nor the reaction network treatment (especially at the branching points) are identical. The multi-event model also presents the advantage of considering T- and N_n-dependent events. Nevertheless, the most fundamental difference between both models lies in the hypothesis of a predefined exposure distribution existing in the classical approach, but abolished in the multi-event method. The neutron exposure distribution characteristic of the multi-event fit is given in Fig. 2 and compared with the exponential form of Beer et al. (1997). Although both models agree qualitatively, it is seen that the deviations from the exponential form derived by the multi-event minimization procedure can improve the fit to the solar abundance of the s-only nuclei. In particular, the weak and strong components predicted by both models are quite different. A more detailed comparison can be found in Goriely (1997).

The multi-event s-process model is now used to decompose the solar abundances of the r- and sr-isotope into their s- and r-components. The resulting solar r-abundance distribution is shown in Fig. 3 and compared with the exponential model predictions of Palme & Beer (1993). For a better understanding, we define here the s-dominant nuclei as sr-nuclei that can be produced by the multi-event s-process by more than 50% of the solar value. Similarly, the r-dominant nuclei are produced by the s-process between 10 to 50% of their solar abundance and the r-only by less than 10%. As seen in Fig. 3, non-negligible deviations between the classical and multi-event models are obtained for the s-dominant $A \lesssim 90$ and $A \gtrsim 204$ nuclei. This result is to be expected, because of the difficulty for the exponential model reliably to determine the characteristic neutron exposures of the weak and strong components. As regards the solar r-abundances in the $90 \lesssim A \lesssim 204$ range, both models globally predict the same abundance distribution, although some small differences are observed for the s-dominant $A \simeq 120$, $A \simeq 140$ and $A \simeq 180$ nuclei.

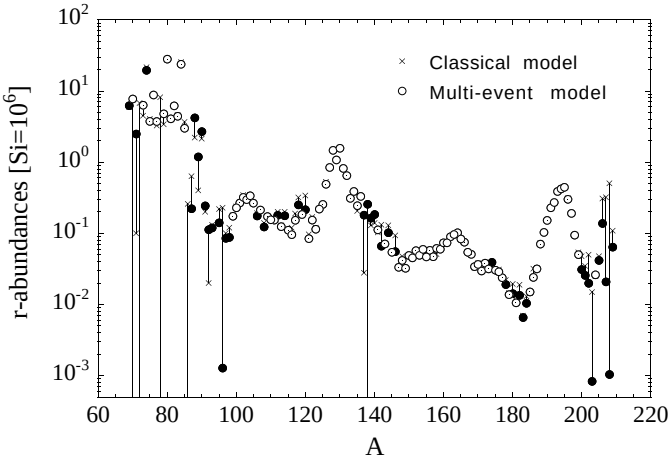

Fig. 3. Comparison of the solar system r-abundances predicted by the exponential model (Palme & Beer 1993) and the multi-event model. Both predictions are connected with a vertical line for the same isotope and normalized to the solar abundance of ^{130}Te. Full, dotted and open circles correspond to s-dominant, r-dominant and r-only nuclei, respectively.

The multi-event s-process developed here also predicts the production of the ^{180}Ta in solar quantity through the β-decay branching at ^{179}Hf, as already explained in Goriely (1997). On the other hand, the s-contribution to other p-nuclei is always negligible, except for ^{114}Sn (10% of the solar value), ^{115}Sn (27%), and ^{180}W (45%).

The multi-event s-process model presented so far is in qualitatively good agreement with the exponential model predic-

tions. This comparison mainly aimed at proving the reliability and predictive power of the multi-event model. Compared with the classical approach, a major advantage of the multi-event approach is to open the way to a possible systematic study of the various uncertainties affecting the parametric s-process model. As a matter of fact, the iterative inversion method works in such a way that the modification of a given (nuclear or astrophysics) input in the s-process model leads to an automatic renormalization of the thermodynamic conditions necessary to optimize the fit to the solar abundance of the s-only isotopes. Therefore, the uncertainties affecting the input data of the parametric model, as well as their impact on the production of the s-only nuclei and the estimate of the residual solar r-abundances, can be studied systematically within the multi-event approach, as shown in the coming section.

3. Uncertainties in the solar system r-abundance distribution

The parametric s-process model plays an important role in estimating the residual r-contribution to the solar system abundances. On the one hand, many sr-nuclei are dominantly produced by the r-process, and consequently their solar abundances are rather insensitive to the calculated s-contribution. On the other hand, other sr-nuclei can be significantly synthesized during the s-process, and their resulting residual solar abundances are this time affected by all astrophysical and nuclear physics uncertainties inherent to the parametric s-process model. The above comparison between the multi-event and classical model emphasizes the sensitivity of the solar r-abundance distribution to the astrophysical modelling of the s-process. Other uncertainties concern principally the remaining inaccuracies in the determination of the isotopic solar system abundances and the nuclear physics input to the s-process model, i.e the radiative neutron capture cross-sections and the β-decay and EC rates. The impact of these various uncertainties are analyzed, first separately, then simultaneously, in the following subsections.

3.1. Uncertainties in observational data

The quality of the observational data is inevitably influenced by the spectroscopic or physico-chemical peculiarities of each species (Anders & Grevesse 1989; Palme & Beer 1993). As already mentioned, we adopt here the abundances (along with their upper and lower limits) prescribed by Palme & Beer (1993). The error bars on the elemental abundances amount from 3 up to 20% (Fig. 4). Three specific elements raise specific problems. These are the non-observable Kr, Xe and the ill-detectable Hg. Since neither meteoritic analyses, nor solar observations are available for these elements, their abundances are so far estimated through interpolation methods with neighbouring isotopes or more lately through theoretical systematics based on the classical s-process model. This latter determination is used in the compilation of Palme & Beer (1993).

To calculate the impact of observational uncertainties on the solar r-abundances, we consider a representative sampling of 10

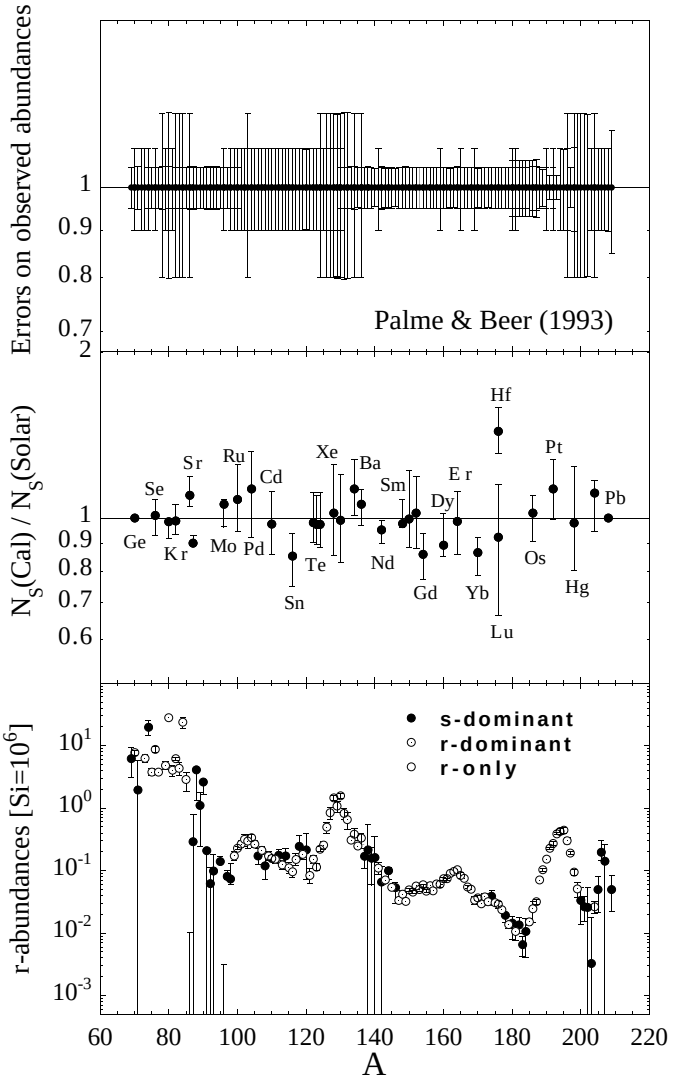

Fig. 4. *Upper panel*: Uncertainties in the observed solar system abundances as given by Palme & Beer (1993). *Middle panel*: Ratio of the multi-event to the solar abundances for the s-only nuclei as given in Fig. 1. The error bars correspond to the impact of the uncertainties in the observed abundances. *Lower panel*: Multi-event prediction of the solar r-abundances as in Fig. 3 with error bars resulting from the uncertainties in the solar abundances. Full, dotted and open circles correspond to s-dominant, r-dominant and r-only nuclei, respectively.

different multi-event calculations, each of them being characterized by a random selection among the upper and lower limits of each elemental solar value. In each case, the iterative method is applied to estimate the best-fit to the solar abundance of the s-only nuclei. The resulting upper and lower limits in the calculated s- and r-abundance distributions are shown in Fig. 4 as error bars around the standard calculation of Sect. 2. Note that none of the 10 fits leads to a deviation larger than $f_{rms} = 1.16$. It is seen that a small uncertainty on the observed abundances (around 5% in average) can have an important influence on the best-fit abundances. As a consequence, the residual solar r-abundance of the s-dominant nuclei show large deviations from the standard predictions, especially in the Ba, La, Ce region and around

the Pb peak. The s-process may indeed be capable to produce the total solar value (at least within the error bars) of isotopes like ^{138}Ba, ^{140}La, ^{142}Ce, so that the derived r-component becomes negligible (Fig. 4). However, it should be stressed that if the s-contribution reaches about 100% of the solar value, the r-component cannot be determined safely anymore by subtracting the s-contribution from the solar abundance, as seen by the very large error bars in the r-abundances of Fig. 4. This feature does not appear for the r-dominant and r-only nuclei the abundance of which remain much less affected.

3.2. Uncertainties in experimental (n,γ) rates

The radiative neutron capture cross-sections have now been measured for almost all the stable nuclei involved in the s-process. The uncertainties in the experimental (n,γ) rates have been highly reduced in recent years reaching in some cases a precision smaller than one or two percents. The remaining uncertainties are illustrated in Fig. 5. Although some large errors around the Xe or Pt isotopes still exist, most of the rates are known within less than 10%. Again, to estimate the impact on the s- and r-abundance distributions, 10 multi-event calculations are performed with a random selection of the neutron capture rates within the prescribed error bars. In each case, a best-fit optimization determines the s-abundances (all the calculations lead to excellent fits with deviation factors smaller than $f_{rms} = 1.17$). The upper and lower values of the s-abundance ratios are shown in the middle panel of Fig. 5. The remaining imprecisions in the experimental (n,γ) rates are seen to have a strong impact on the s-process predictions, as already well established (Käppeler et al. 1989). However, it is of importance to stress the non-linear dependence of this impact. For example, errors larger than 10% are found in the ^{134}Ba and ^{136}Ba abundances, though only a 3% error exists in the neutron capture rates of the Ba isotopes. This effect is essentially due to the non-local property of the fitting procedure, i.e the global root mean square deviation is minimized without constraining the fit to any particular mass region. Consequently, a decrease of a temperature-dependent rate can, for example, be compensated by an increase of the characteristic (i.e "best-fit") temperature of the s-process which in turn can modify other reaction rates and therefore the predicted abundances. Since in the 10 fits considered, the rms deviation is very low ($f_{rms} < 1.17$) and no particular nucleus is exaggeratedly overproduced, all the "best-fit" solutions found can be considered as physically plausible. In this case, the error bars do indeed depict the real sensitivity of the s-abundances to the studied uncertainties.

Note that in addition to the unavoidable experimental errors, there exists another source of uncertainty in the (n,γ) rates which can become significant, especially in view of the high precision obtained now-a-days in the measurements. This concerns the stellar enhancement factor due to the contribution of thermally populated low-lying states in the target nucleus. It is the case for the (n,γ) reactions on the s-only isotopes ^{160}Dy, ^{164}Er, ^{170}Yb, ^{176}Hf and ^{187}Os, the rates of which have been experimentally determined within a few percent (Beer et al. 1992, Wisshak et al, 1998). The stellar cross sections are estimated by the code MOST to differ from the laboratory value by +10, 19, 16, 20 and 37%, respectively. Even though this thermalization factor only represents a small correction (10-20%) on some reaction rates, it remains quite significant in comparison to the characteristic experimental errors prescribed in the literature. These corrections tend to decrease the predicted s-abundances. Some 25 experimentally-known (n,γ) reaction rates on s-dominant or r-dominant nuclides are also found to be affected within 10 to 40% by the specific conditions of the stellar environment. These effects can modify some solar r-abundances, as already shown in Goriely (1997). The determination of the stellar enhancement factor depends mainly on the nuclear level density prescription and is also bound to theoretical uncertainties. MOST enhancement factors have been considered for all laboratory measurements, but only uncertainties of experimental origin have been considered here.

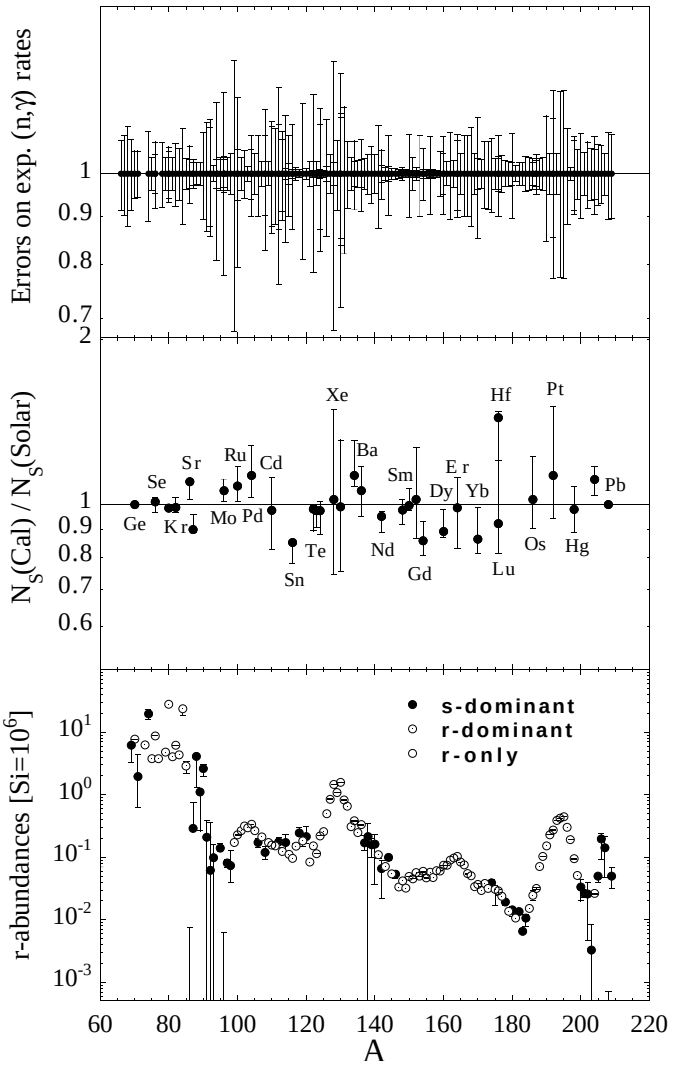

Fig. 5. Same as Fig. 4 for the uncertainties in the experimental radiative neutron capture rates.

3.3. Uncertainties in theoretical (n, γ) rates

Theoretical evaluations of the neutron capture rates refer to unstable nuclei for which no experimental measurement is available at the present time. Theoretical estimates within the HF model are known to be reliable within a factor of 2 to 3 for nuclei close to the β-stability valley (Thielemann et al. 1986). However, HF predictions still suffer from uncertainties associated with the predictions of the nuclear level density, the photon transmission coefficient and the nucleon-nucleus potential. Updates as well as improvements have been brought to the HF code, called MOST, dedicated to astrophysical applications (Goriely 1998b). MOST includes all experimental data available on nuclear masses, deformations, spectra of low lying states, giant dipole energies and widths. Information on neutron resonance spacings at the neutron separation energies is also introduced to normalize the microscopic model of nuclear level densities (Goriely 1996). Such experimental information is fundamental for an optimum prediction of neutron capture rates as required in s-process calculations.

When the nuclear ingredients to the HF model cannot be determined from experimental data, MOST uses semi-microscopic predictions based on sound and reliable nuclear models which can compete in the reproduction of experimental data with phenomenological highly-parametrized models. In particular, the ETFSI model (Aboussir et al. 1995) of nuclear masses, density distributions and deformations is a key ingredient in MOST. MOST also makes use of a NLD formula based on the microscopic treatment of the partition function method (Goriely 1996). Improvements brought to MOST also concern the description of the giant dipole resonance strength function at low energies (Goriely 1998a). As regards the neutron-nucleus potential, MOST uses the Brueckner-Hartree-Fock approximation of Jeukenne et al. (1977). Note that in addition to these above-mentioned models, other prescriptions of the nuclear structure properties (e.g Hilf et al. 1976), nuclear level densities (e.g Thielemann et al. 1986; Rauscher et al. 1997), dipole resonance characteristics (e.g Thielemann et al. 1986) and optical potentials (e.g Bauge et al. 1998) are commonly available in the literature and enable us to estimate the sensitivity of the calculated cross-sections to different HF inputs. Twelve different combinations of the above-cited inputs were used to evaluate upper and lower limits to the experimentally-unknown neutron capture rates. Fig. 6 shows the resulting deviations on the neutron capture rates from our standard MOST predictions for 189 unstable nuclei involved in the s-process. It is seen that MOST predictions can correspond to the upper or lower values compared with calculations obtained with a modified input. Globally, the HF rates deviate by an average ratio of about 5 between the upper and lower values, although some reactions appear to be affected by a much larger value. This deviation factor is in agreement with the usual statement that the HF predictions are reliable within a factor of 2. Nevertheless, it should be stressed that the HF calculation performed here is a global one and is not fine-tuned in any particular mass region. It remains difficult to use local optimizations of the HF predictions in our systematic

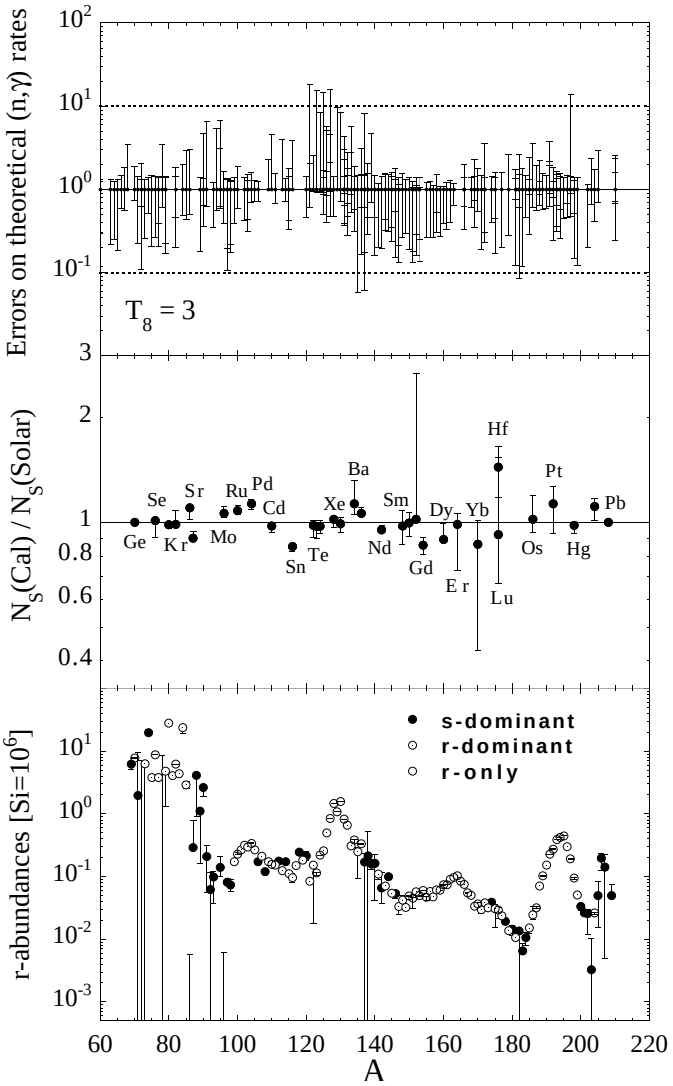

Fig. 6. Same as Fig. 4 for the uncertainties in the theoretical radiative neutron capture rates. The *upper panel* shows such uncertainties for 189 unstable nuclei involved in the s-process at the temperature $T_8 = 3$.

study of nuclear uncertainties affecting the s-process. Moreover, even if each ingredient of the HF calculation is chosen to reproduce known experimental data, a unique extrapolation to unknown mass or energy regions is not necessary obtained. In particular, the microscopic and Back-shifted Fermi gas model can lead to different energy dependence of the level density, and therefore predictions of the reaction rates.

A random choice among upper and lower HF predictions is used in 10 different multi-event calculations. The best-fit minimization in each case gives the error bars on the s-abundances that are illustrated in Fig. 6. The elements lighter than Ba are almost unaffected by theoretical uncertainties. This means that the local approximation $N(Z, A)\langle\sigma\rangle = \text{constant}$ (where $\langle\sigma\rangle$ is the Maxwellian-averaged neutron capture cross-section) is well fulfilled. For elements heavier than Ba, branching points come into play. Different predictions of their capture rate lead to modifications in the predicted abundance of the s-only elements. This

is the case for ^{152}Gd (which might not be by-passed any more by the ^{151}Sm or ^{152}Eu branchings) or ^{170}Yb (depending on the $^{170}\mathrm{Tm}(n,\gamma)^{171}\mathrm{Tm}$ rate uncertain within a factor of 3). Fig. 6 emphasizes the need of theoretical improvements for given rates (and in particular, for the above-mentioned ones).

The impact of the studied theoretical uncertainties on the solar r-abundance distribution is also illustrated in Fig. 6. In particular, the r-dominant ^{122}Sn can be produced in a larger amount by the s-process (leading to a lower solar r-component) if use is made of the upper value of $^{121}\mathrm{Sn}(n,\gamma)^{122}\mathrm{Sn}$ rate obtained with the level density formula of Thielemann et al. (1986) and the optical potential of Bauge et al. (1998). A large uncertainty also affects the r-contribution to the ^{182}W solar abundance. A smaller capture rate on the pre-sitting branching nuclei ^{181}Hf and ^{182}Ta causes an increase of the ^{182}W s-component up to 100% of the solar value. In this case, the r-component of the ^{182}W solar abundance is ill-defined. Similar conclusions are found in the Ge, Ba and Pb regions.

3.4. Uncertainties in β-decay and EC rates

In addition to the uncertainties plaguing the neutron capture rates, weak interaction properties also face some theoretical problems. Although all the β-decay and EC rates of relevance in the s-process modelling are known in terrestrial conditions, the contribution of thermally populated excited states, as well as atomic effects in the strongly ionised stellar plasma can drastically modify the laboratory value (Yokoi & Takahashi 1987). The calculated β-rates in stellar environments are subject to nuclear uncertainties which remain difficult to estimate. The uncertainties in the stellar β-decay and EC rates strongly depend on the relevance of the experimentally unknown transitions at a given temperature and density and the reliability of their evaluated probability. Only a systematic estimate of the rates as done by Yokoi & Takahashi (1987) can give a precise idea about the resulting temperature- and density-dependent errors. To do so, we have reiterated the Yokoi & Takahashi (1987) calculation with unknown transition rates modified by a typical error value of $\log ft = \pm 0.5$ (Takahashi 1998, private communication). Note that no transition faster than $\log ft = 5$ is permitted in this error calculation and that newly measured transition probabilities, e.g the allowed transition in the ^{187}Re bound-state β-decay (Bosch et al. 1996), have been considered. Minimum and maximum error factors around the published rates of Yokoi & Takahashi (1987) are given in Fig. 7 at $T_8 = 3$ and $N_e = 10^{27}\,\mathrm{cm}^{-3}$ and in a table format in Tables 1 and 2 at other temperatures and electronic densities (expressed in terms of $10^{26}\,\mathrm{cm}^{-3}$). When the density-dependence does not affect the final uncertainty factor by more than 0.10 between the $N_e = 10^{26}$ and $3\,10^{27}\,\mathrm{cm}^{-3}$ cases, only values at $N_e = 10^{27}\,\mathrm{cm}^{-3}$ are given in the tables. Note that an increase of transition probability by $\log ft = 0.5$ gives rise to an increase of the final rate by a maximum value of 3.16. This maximum variation is obtained for many rates.

The influence of uncertain weak rates is analyzed by performing, once again, 10 multi-event s-process calculations with 10 different random choices among the upper and lower limits of the β-rates. The best-fit to the s-only abundances along with the corresponding error bars is shown in Fig. 7. Only a few s-only isotopes are affected, namely ^{104}Pd, ^{134}Ba, ^{152,154}Gd, ^{160}Dy, ^{164}Er, ^{176}Lu and ^{176}Hf. The impact on the derived solar r-abundances is nevertheless small (Fig. 7).

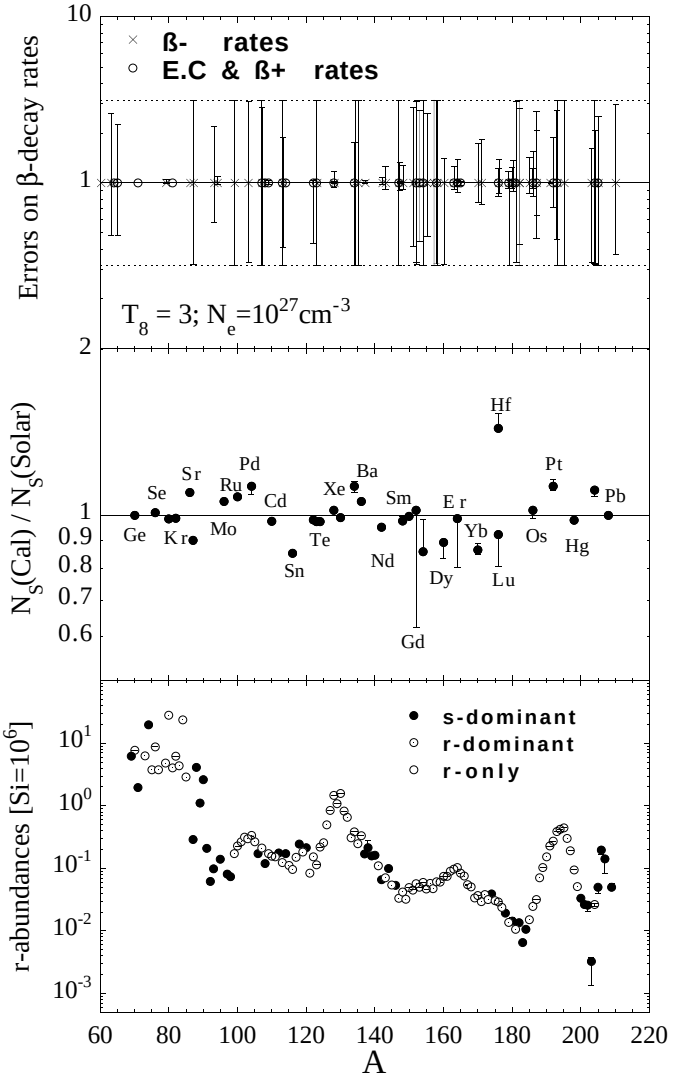

Fig. 7. Same as Fig. 4 for the uncertainties in the β-decay and EC rates.

3.5. Final uncertainties in the solar s- and r-abundance distributions

We now consider, simultaneously, the 4 types of uncertainties studied separately in the previous subsections. 20 multi-event s-process calculations are performed allowing for upper and lower values of the observed abundances, experimental and HF (n,γ) rates and β-decay rates. In the 20 cases, the deviation factor f_{rms} resulting from the best-fit procedure is found to be small reaching a maximum value of 1.30. Before analyzing the impact of the combined uncertainties, it should be mentioned that the nucleosynthesis in the particular Pb region presents a special complication and that the error bars in this region might

be underestimated. The s-process is known to be able to produce the Pb and Bi isotopes in large quantities. This result is obviously bound to the assumption that irradiations with values of n_{cap} as high as 150 (or $\tau \simeq 2$ mb^{-1}) are effectively found in astrophysical environments. Lower values would obviously give rise to a smaller s-contribution, and consequently to a larger r-component. Both the s- and the r-processes are able to produce the Pb-Bi isotopes in almost solar abundance. Unfortunately, our poor understanding of the astrophysical scenarios in which they take place, as well as the complex nuclear physics properties of the heaviest nuclei in the actinide region affecting the r-process nucleosynthesis, does not allow us to favour one particular nucleosynthetic mechanism. For this reason, we also consider the multi-event model predictions in which the so-called strong component of the s-process is suppressed. To do so, the s-process is assumed to take place with a number of neutrons captured per seed nuclei that does not exceed $n_{cap}^{max} = 85$. This maximum value of n_{cap} enables a possible solar production of the heaviest s-only isotope ^{204}Pb without deteriorating the qualilty of the global fit to the s-only (note that in this case the fit is obviously not constrained by the solar abundance of ^{208}Pb anymore). In a similar way as mentioned above, 20 muli-event s-process calculations are reiterated under these conditions allowing for a random selection among the upper and lower limits of the 4 type of uncertainties.

The impact of the final (i.e resulting from the 40 multi-event calculations as explained above) combined uncertainties on the fit to the abundances of the s-only elements is shown in Fig. 8 along with the resulting solar r-abundance distribution. The combined uncertainties are seen to have striking effects. For example, in the case of ^{134}Ba, the lower limit of its solar value associated with a slower β-decay rate of and a faster neutron capture rate on ^{134}Cs (within the error limits) lead to an impressive underestimate of the solar value. Except for ^{176}Hf, the solar abundance of all the s-only isotopes can be understood in terms of the multi-event model, i.e thermodynamic conditions and exposure times can be found within the canonical model that give rise to the production of each s-only nucleus in solar abundance, at least within the uncertainties described in the present paper. The large error bar in ^{208}Pb reflects the possible absence of a strong component in the s-process.

The final uncertainties in the predicted s-abundances are responsible for the large variations found in the solar r-abundances (Fig. 8 and Table 3). Most of the s-dominant nuclei can be produced entirely by the s-process, and therefore present an r-component of the solar abundance with a large error bar. More particularly, the abundances in the Pb region are affected by large uncertainties due not only to observational and nuclear data, but also to the possible lack of strong neutron irradiations in astrophysical environments which could produce ^{204}Pb in solar abundance but not ^{208}Pb. This problematic aspect of the abundance splitting in the Pb region makes the solar r-abundances in the Pb peak an unreliable set of data for basing r-process extrapolation up to the actinide region.

The corresponding elemental r-abundance distribution including the studied uncertainties is shown in Fig. 9. It is seen

Table 3. Standard, minimum and maximum r-contributions to the solar system abundances N(Z,A) relative to 10^6 Si atoms.

Z	A	Stand	Min	Max	Z	A	Stand	Min	Max
31	69	6.1800	0.0000	9.3700	58	140	0.1610	0.0000	0.3570
30	70	7.7400	6.8000	8.5500	59	141	0.1100	0.0545	0.1360
31	71	1.9600	0.0000	9.6100	58	142	0.0660	0.0000	0.1310
32	72	0.0000	0.0000	9.9300	60	143	0.0706	0.0526	0.0811
32	73	6.3100	0.0000	8.1900	60	144	0.0998	0.0582	0.1240
32	74	19.700	9.9400	28.900	60	145	0.0540	0.0456	0.0611
33	75	3.7800	3.2400	4.6800	60	146	0.0533	0.0145	0.0711
32	76	8.7800	7.8400	9.6800	62	147	0.0334	0.0156	0.0347
34	77	3.7600	3.4800	4.6500	60	148	0.0421	0.0221	0.0522
34	78	0.0000	0.0000	10.300	62	149	0.0323	0.0278	0.0328
35	79	4.8100	0.9180	5.7100	60	150	0.0490	0.0459	0.0515
34	80	28.100	24.800	32.200	63	151	0.0452	0.0267	0.0482
35	81	4.0700	3.0400	4.8700	62	152	0.0571	0.0498	0.0622
34	82	6.2000	5.8300	6.5100	63	153	0.0495	0.0460	0.0526
36	83	4.3800	3.0500	5.6800	62	154	0.0595	0.0505	0.0609
36	84	23.600	14.200	34.500	64	155	0.0468	0.0364	0.0500
37	85	2.8700	1.0500	4.0100	64	156	0.0579	0.0501	0.0634
36	86	0.0000	0.0000	0.5870	64	157	0.0471	0.0429	0.0508
37	87	0.2920	0.0000	1.0100	64	158	0.0614	0.0497	0.0694
38	88	4.0900	0.0000	4.7500	65	159	0.0601	0.0517	0.0672
39	89	1.1100	0.0000	1.8100	64	160	0.0741	0.0655	0.0787
40	90	2.6100	1.2600	3.0100	66	161	0.0741	0.0684	0.0745
40	91	0.2100	0.0000	0.4840	66	162	0.0900	0.0795	0.0917
40	92	0.0620	0.0000	0.4370	66	163	0.0972	0.0890	0.0980
41	93	0.0987	0.0000	0.2700	66	164	0.1030	0.0827	0.1040
40	94	0.0000	0.0000	0.0602	67	165	0.0839	0.0728	0.0941
42	95	0.1400	0.0976	0.2260	68	166	0.0753	0.0691	0.0833
40	96	0.0000	0.0000	0.0250	68	167	0.0546	0.0495	0.0586
42	97	0.0808	0.0496	0.1120	68	168	0.0506	0.0420	0.0570
42	98	0.0739	0.0000	0.1530	69	169	0.0340	0.0250	0.0391
44	99	0.1730	0.1460	0.2000	68	170	0.0369	0.0283	0.0407
42	100	0.2260	0.2100	0.2500	70	171	0.0297	0.0107	0.0326
44	101	0.2670	0.2300	0.3050	70	172	0.0381	0.0323	0.0432
44	102	0.3150	0.2440	0.4260	70	173	0.0316	0.0266	0.0353
45	103	0.2970	0.2090	0.3750	70	174	0.0391	0.0229	0.0515
44	104	0.3370	0.2980	0.3830	71	175	0.0305	0.0156	0.0374
46	105	0.2660	0.2240	0.3030	70	176	0.0292	0.0177	0.0334
46	106	0.1710	0.1130	0.2280	72	177	0.0238	0.0186	0.0263
47	107	0.2110	0.1780	0.2440	72	178	0.0192	0.0100	0.0236
46	108	0.1190	0.0660	0.1930	72	179	0.0138	0.0109	0.0160
47	109	0.1720	0.1310	0.2070	72	180	0.0145	0.0000	0.0214
46	110	0.1560	0.1360	0.1740	73	181	0.0106	0.0042	0.0144
48	111	0.1520	0.1270	0.1790	74	182	0.0136	0.0000	0.0215
48	112	0.1760	0.0921	0.2500	74	183	0.0065	0.0000	0.0100
48	113	0.1240	0.0916	0.1550	74	184	0.0106	0.0000	0.0179
48	114	0.1720	0.0515	0.2910	75	185	0.0151	0.0110	0.0176
49	115	0.1110	0.0816	0.1360	74	186	0.0245	0.0073	0.0337
48	116	0.0955	0.0697	0.1270	75	187	0.0318	0.0270	0.0359
50	117	0.1500	0.1030	0.1930	76	188	0.0708	0.0633	0.0781
50	118	0.2440	0.1510	0.3750	76	189	0.1030	0.0961	0.1090
50	119	0.1840	0.1150	0.2470	76	190	0.1520	0.1370	0.1680
50	120	0.2140	0.0634	0.4120	77	191	0.2290	0.2210	0.2370
51	121	0.0836	0.0578	0.1130	76	192	0.2730	0.2520	0.2890
50	122	0.1520	0.0000	0.1800	77	193	0.3880	0.3740	0.4020
51	123	0.1130	0.0925	0.1310	78	194	0.4210	0.3620	0.4700
50	124	0.2200	0.1950	0.2420	78	195	0.4450	0.3940	0.4930
52	125	0.2560	0.2170	0.2950	78	196	0.3020	0.2560	0.3470
52	126	0.4920	0.3810	0.6010	79	197	0.1910	0.1790	0.2040
53	127	0.8480	0.6630	1.0300	78	198	0.0950	0.0805	0.1050
52	128	1.4700	1.2900	1.6200	80	199	0.0507	0.0357	0.0682
54	129	1.0800	0.8510	1.3100	80	200	0.0334	0.0061	0.0640
52	130	1.5800	1.4200	1.7400	80	201	0.0265	0.0111	0.0426
54	131	0.8220	0.6270	1.0100	80	202	0.0257	0.0000	0.0677
54	132	0.6530	0.3890	0.9260	81	203	0.0033	0.0000	0.0271
55	133	0.3090	0.2830	0.3410	80	204	0.0266	0.0171	0.0330
54	134	0.3850	0.2310	0.4770	81	205	0.0497	0.0000	0.1150
56	135	0.2480	0.0000	0.2720	82	206	0.1970	0.0364	0.3790
54	136	0.3300	0.2600	0.3960	82	207	0.1420	0.0000	0.4330
56	137	0.1700	0.0000	0.2960	82	208	0.0003	0.0000	1.7800
56	138	0.2140	0.0000	1.0000	83	209	0.0501	0.0100	0.1640
57	139	0.1570	0.0183	0.2480					

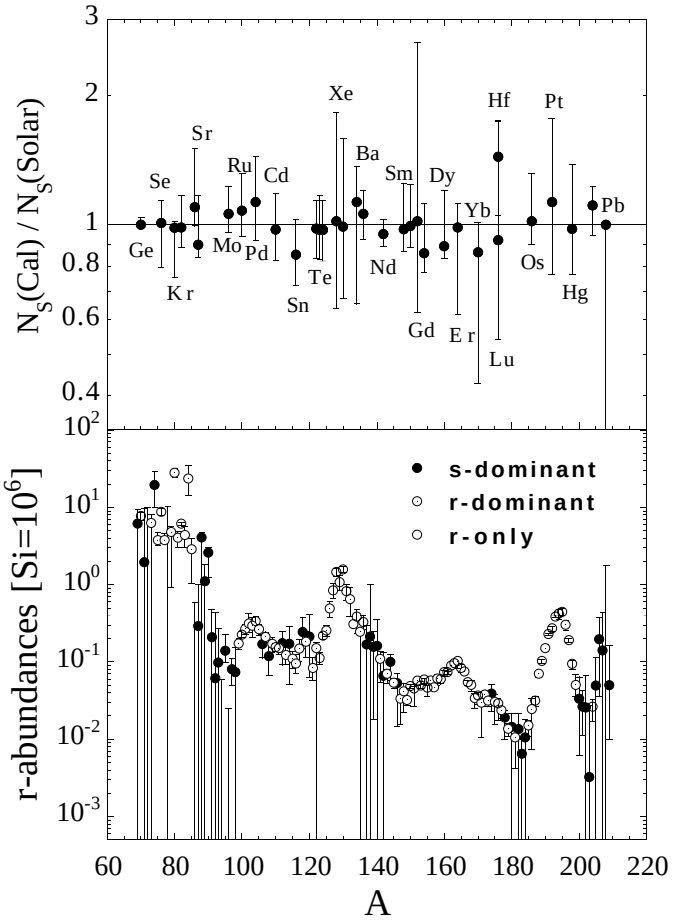

Fig. 8. *Upper panel*: Ratio of the multi-event to the observed abundances for the s-only nuclei as given in Fig. 1. The error bars correspond to the impact of all the uncertainties studied simultaneously (including those related to the strong s-process component). *Lower panel*: Solar r-abundances with error bars resulting from the uncertainties found in the *upper panel*. Full, dotted and open circles correspond to s-dominant, r-dominant and r-only nuclei, respectively.

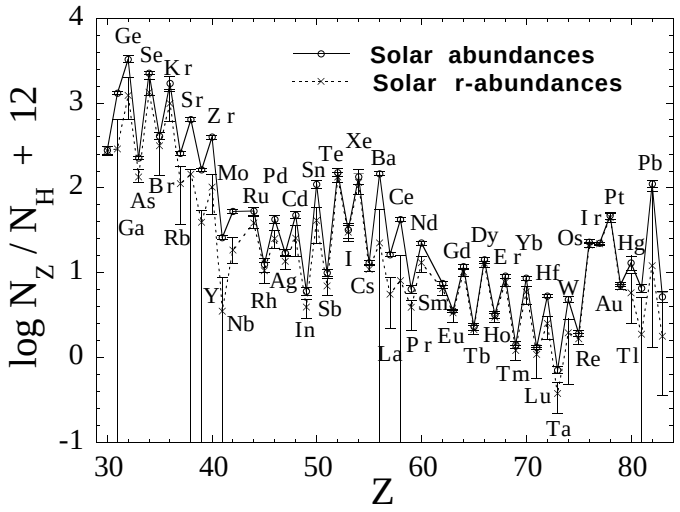

Fig. 9. Elemental solar r-abundances (dash line) with error bars resulting from all the studied uncertainties, expressed in units normalized to 10^{12} H atoms. Also shown are the total solar system abundances (full line).

that the r-contribution to the solar abundance of nuclei, such as Rb, Sr, Y, Zr and Ba, La, Ce, is not known with a high degree of accuracy. Unfortunately, some of these elements, in particular Ba, are often used as observational tracers to identify s- or r-process contents in the stellar photosphere. This feature does not facilitate our understanding concerning the pollution of s-origin elements in ultra-metal-poor stars enriched in r-elements (Sneden et al. 1996).

4. Conclusions

The parametric s-process model plays an important role not only in trying to explain the nuclear mechanisms taking place during the s-process, but also in deriving the residual r-contribution to the solar system abundances. The parametric s-process approach followed in the present paper is called the multi-event model and is based on an optimized superposition of s-process events at different temperatures and neutron densities which reproduces the solar system s-content as precisely as possible. The multi-event model is shown to give an excellent fit to the solar system abundances of the s-only nuclei. When compared with the traditional exponential model, the multi-event model emphasizes how the fit to the solar abundances of the s-only nuclei, as well as the solar r-abundance distribution is sensitive to the assumption made in the exponential model regarding the pre-defined exposure distribution. Moreover, the multi-event model provides a unique tool to study the impact of the remaining nuclear and astrophysics uncertainties on the solar s- and r-abundance distributions. The modification of a given input to the multi-event model leads to a renormalization of the thermodynamic conditions necessary to optimize the fit to the solar abundances of the s-only isotopes. Therefore, performing various multi-event calculations with different input data enables us to estimate the impact of the remaining uncertainties not only on the s-process nucleosynthesis, but also on the residual solar r-abundances.

Making use of this property of the multi-event model, the major uncertainties affecting the prediction of the s-abundance distribution are studied in detail. Observational and nuclear uncertainties are estimated. In particular, a detailed calculation is made to evaluate the impact of different nuclear input to the HF reaction rate. Temperature- and density-dependent error factors are also derived for the β-decay and EC rates in a consistent way. The impact of such uncertainties on the solar s- and r-abundance distributions are analyzed separately and simultaneously. It is found that the remaining error bars in the observed meteoritic abundances and in the relevant (n,γ) rates influence the predicted s-component of the solar abundance in a non-negligible way. The residual solar r-abundances is consequently affected, especially as far as the s-dominant nuclei are concerned. Uncertainties in theoretical predictions of the neutron capture and β-decay rates have a smaller impact on the nucleosynthesis calculations, though the combination of these uncertainties can affect the s-production of the heaviest $A \gtrsim 134$ nuclei in a significant

way. When considered all simultaneously, the remaining uncertainties appear to be such that all the solar abundances of the s-only nuclei can be explained satisfactorily. The resulting uncertainties in the s-component of the solar abundance give rise to large errors in the solar r-abundances of the s-dominant isotopes. Minimum and maximum values of the solar r-component are tabulated. These error bars on the r-abundance distribution should be taken into account when comparing observed or calculated r-process abundances with the solar system content.

Finally, it should be recalled that other uncertainty factors in the s-modelling have not been considered here and could also exert influence on the splitting of the solar abundances into their s- and r-components. These mainly concern uncertainties inherent to the assumptions made in the canonical approach of the s-process, i.e. the seed abundance distribution, the range of thermodynamic conditions to be considered and the time-independent thermodynamic profiles. A future work will consist in studying the effects associated with time-dependent profiles of the neutron density resulting from the neutron sources $^{13}\mathrm{C}\,(\alpha\,,\mathrm{n})\,^{16}\mathrm{O}$ or $^{22}\mathrm{Ne}\,(\alpha\,,\mathrm{n})\,^{25}\mathrm{Mg}$ in a given range of temperatures and densities.

Acknowledgements. The author is grateful to K. Takahashi for helpful discussions and providing the mean of calculating the β-decay rates. S.G. is F.N.R.S. Senior Research Assistant.

References

Aboussir Y., Pearson J.M., Dutta A.K., Tondeur F., 1995, At. Data Nucl. Data Tables 61, 127
Anders E., Grevesse N., 1989, Geochim. Cosmochim. Acta 53, 197
Arnould M.,1976, A&A 46, 117
Arnould M., Takahashi K., 1998, Rep. Prog. Phys. in press
Bao Z.Y., Käppeler F., 1987, At. Data Nucl. Data Tables 36, 411
Bauge, E., Delaroche, J.P., Girod, M., 1998, Phys. Rev C in press.
Baraffe I., El Eid M.F., Prantzos N., 1992, A&A 258,357
Beer H., Voss F., Winters R.R., 1992, ApJS 80, 403
Beer H., Corvi F., Mutti P., 1997, ApJ 474, 853
Bosch F., Faestermann, T., Friese, J., 1996, Phys. ReV. Lett. 77, 5190
Burbidge E.M., Burbidge G.R., Fowler W.A., Hoyle F., 1957, Rev. Mod. Phys. 29, 547
Busso M., Gallino R., Lambert D.L., Raiteri C.M., Smith V.V., 1992, ApJ 399, 218
Clayton D.D., Fowler W.A., Hull T.E., Zimmerman B.A., 1961, Ann. Phys. 12, 331
Frost C.A., Lattanzio J.C., 1995, In: Noels A., Fraipont-Caro D., Gabriel M., Grevesse N., Demarque P. (eds) Stellar Evolution: What should be done. Proc. of the 32nd Liège International Astrophysical Colloquium, p.307
Goriely S., 1996, Nucl. Phys. A605, 28
Goriely S., 1997, A&A 327, 845
Goriely S., 1998a, Phys. Lett. B in press.
Goriely S., 1998b, In: Proceedings of the international conference on Nuclei inthe Cosmos (Volos, Greece) in press.
Hilf E.R., von Groote H., Takahashi K., 1976, In: Proc. Third International Conference on Nuclei far from Stability (CERN 76-13, Geneva), 142
Jeukenne, J.P., Lejeune, A., Mahaux, C., 1977, Phys. Rev C16, 80
Hollowel D.E., Iben I. Jr., 1989, ApJ 340, 966
Käppeler F., Beer H., Wisshak K., 1989, Rep. Prog. Phys. 52, 945
Langer N., Arcoragi J.P., Arnould M., 1989, A&A 210, 187
Lattanzio J.C., 1989, In: Johnson H.R., Zuckerman B. (eds.) Evolution of Peculiar Red Giants, CUP, p.161
Malaney R.A., Boothroyd A.I., 1987, ApJ 320, 866
Nemeth Zs., Käppeler F., Theis C., Belgya T., Yates S.W., 1994, ApJ 426, 357
Palme H., Beer H., 1993, In Landolt Börnstein, New Series, Group VI, Astronomy and Astrophysics, Subvolume 3a, Springer, Berlin, p.196
Prantzos N., Hashimoto M., Nomoto K., 1990 A&A 234, 211
Qian Y.-Z., Woosley S.E., 1996, ApJ 471, 331
Rauscher, T., Thielemann, F.-K., Kratz, K.-L., 1997, Phys. Rev. C56, 1613
Rayet M., El Eid, M. Arnould M., 1993, In: Käppeler F., Wisshak K. (eds) Nuclei in the Cosmos. Institute of Physics Publishing, Bristol, p.613
Rayet M., Arnould M., Hashimoto M., Prantzos N., Nomoto K., 1995, A&A 298, 517
Seeger P.A., Fowler W.A., Clayton D.D., 1965, ApJS 11, 121
Sneden C., Mc William A., Preston G.W. et al, 1996, ApJ 467, 819
Straniero O., Gallino R., Busso M. et al., 1995, ApJ 440, L85
Takahashi K., Yokoi K., 1987, At. Data Nucl. Data Tables 36, 375
Takahashi K., Janka H.-Th., 1997, In: Kajino T., Kubono S. Yoshii Y. (eds) Origin of Matter and Evolution of Galaxies (Singapore: World Scientific), p.213
Thielemann F.-K., Arnould M., Truran J.W., 1986, In: Vangioni-Flam E. et al. (eds.) Advances in Nuclear Astrophysics. Editions Frontières, Gif-sur-Yvette, p.525
Wisshak K., Voss F., Käppeler F. et al., 1995, Phys. Rev C52, 2762
Wisshak K., Voss F., Theis C. et al., 1996, Phys. Rev C54, 1451
Wisshak K., Voss F., Arlandini C. et al., 1998, In: Proceedings of the international conference on Nuclei inthe Cosmos (Volos, Greece) in press.